Removal of Cadmium by Silver Nanoparticles Incorporated in Electrospun Natural Rubber Latex/Polyvinyl Alcohol Matrix*

[1]L. B. Osei*, [1]S. Fosu, and [1]S. A. Ndur
[1]University of Mines and Technology, Box 237, Tarkwa, Ghana

Abstract

In this study, the efficiency of silver nanoparticles (AgNP) incorporated into electrospun natural rubber latex/polyvinyl alcohol (NRL/PVA) nanofibre matrix to remove Cd^{2+} from aqueous solution was examined. Electrospun AgNP-NRL/PVA nanofibre composites were produced using silver nitrate ($AgNO_3$) concentrations of 0.01 M and 0.015 M. Maximum Cd^{2+} was adsorbed at pH 7 for both nanofibre composites but at different reaction times of 20 min for 0.01 M AgNP and 40 min for 0.015 M AgNP. The maximum adsorption for 0.01 M AgNP was 14.9674 mg/g and 30.1129 mg/g for 0.015 M AgNP. Adsorption data were tested with Langmuir, Freundlich and Dubinin-Radushkevich (D-R) isotherms as well as pseudo-first order (PFO), pseudo-second order (PSO), Elovich and intra-particle diffusion kinetic models. Cadmium adsorption by both nanofibre composites fitted best to Freundlich isotherm. Adsorption data for 0.01 M AgNP fitted best to PFO kinetic model, whilst that of 0.015 M AgNP fitted best to Elovich kinetic model, with 0.015 M AgNP having a lower desorption constant and larger boundary layer (β = 0.1793 g/mg; C = 7.5959 mg/g) than 0.01 M AgNP (β = 1.0351 g/mg; C = 4.5942 mg/g). The nanofibre, 0.015 M AgNP, fitting best to Freundlich isotherm and Elovich kinetic model, showed that Cd^{2+} was chemisorbed. In general, 0.015 M AgNP was more efficient in adsorbing Cd^{2+} than 0.01 M AgNP. After the adsorption process, silver (Ag) concentration in the treated water (0.01 M AgNP = 0.0425 mg/L, 0.015 M AgNP = 0.0510 mg/L) was below US EPA and WHO guidelines of 0.10 mg/L for both nanofibre composites, rendering the treated water good enough for human use. Therefore, this work has shown the potential of AgNP incorporated in an electrospun NRL/PVA nanofibre matrix to remove contaminants (Cd^{2+}) from contaminated water.

Keywords: Silver Nanoparticles, Cadmium Adsorption, Natural Rubber Latex, Polyvinyl Alcohol, Electrospun Nanofibre

1 Introduction

Cadmium (Cd^{2+}) is a heavy metal with no known biological function to the human body but has detrimental health effects when cadmium-contaminated water is consumed (Mahmood *et al.*, 2019). Due to Cd^{2+}'s bioaccumulative nature, chronic exposure to low concentrations is considered harmful. Ingesting acute doses of Cd^{2+} can cause gastrointestinal tract erosion, hepatic dysfunction and kidney damage (Tchounwou *et al.*, 2012). Long-term exposure may lead to Itai-Itai disease, which is characterised by softening of the bones and severe bone pain (Aoshima, 2016).

Cadmium is released into water bodies through corrosion of galvanised water supply pipes, desorption from some plastic water supply pipes, municipal landfill leachates, runoff from the application of Cd-laden fertilisers and pesticides, and effluents from mining and smelting sites (Elkhatib *et al.*, 2016; Salehi *et al.*, 2017; Mahmood *et al.*, 2019). Although humans are mostly exposed to Cd^{2+} through food consumption (Anon., 2011), Cd^{2+} in runoff and irrigation waters and aquatic bodies settle in soils and sediments (Aoshima, 2016; Elkhatib *et al.*, 2016; Balali-Mood *et al.*, 2021). Cadmium is assimilated by plants such as leafy vegetables, seeds, grains and potatoes, which is subsequently consumed by humans (Aoshima, 2012; Tchounwou *et al.*, 2012; Aoshima, 2016).

This shows that Cd^{2+} ingested by humans can be limited mainly by reducing Cd-laden effluent release and Cd^{2+} concentration in irrigation water.

Treating contaminated water containing low concentrations of Cd^{2+} is challenging, particularly in countries with lax regulations on Cd^{2+} discharge. Cadmium can be removed from wastewater using techniques such as ion exchange and tight membrane filtration. However, these methods require large quantities of chemicals for resin regeneration, and since the membranes are prone to fouling, it leads to high operational costs (Colantonio and Kim, 2016). It is, therefore, not cost-effective to use these advanced methods to treat Cd^{2+} at low concentrations (Colantonio and Kim, 2016).

In recent years, nanoparticles have proven superior to their bulk counterparts in removing heavy metals from water (Shao-Feng *et al.*, 2005; Kango and Kumar, 2016; Tavker *et al.*, 2021). For instance, silver nanoparticles (AgNP) have the potential to adsorb Cd^{2+} efficiently from water (Al-Qahtani, 2017). However, a pressing challenge is that nanoparticles mostly remain in treated water after the removal of contaminants. Due to the toxicological nature of nanoparticles, having these nanoparticles in treated water is not advisable (Sahu and Hayes, 2017; Pietroiusti *et al.*, 2018). Furthermore, removing AgNP from the treated

water will require additional investment, rendering the whole treatment process expensive (Roksana, 2016). Also, ingesting excess silver (Ag) (that is, AgNP in the treated water) can lead to argyria, which is the discolouration of the dermis and some organs (Han *et al.*, 2011). In view of this, it is necessary to apply AgNP in water treatment when the nanoparticles are incorporated into a matrix. However, some matrices used are mostly micro or nanoparticles, which would need micro or ultrafiltration for final separation (Elkhatib *et al.*, 2016; Tauanov *et al.*, 2019). Given this, it would be plausible to incorporate AgNP into a matrix such as nanofibres since this material is large enough to be separated from treated water using conventional filtration.

The potential of AgNP in electrospun nanofibre matrices like natural rubber latex/polyvinyl alcohol (NRL/PVA) to adsorb metals such as Cd^{2+} has not been explored. Therefore, this study aims to investigate the efficiency of AgNP in NRL/PVA nanofibre (AgNP-NRL/PVA nanofibre composites) to sorb or remove Cd^{2+} from an aqueous solution. In the sorption experiments, the main parameters considered were pH, contact time and initial concentration of Cd^{2+}.

2 Resources and Methods Used

2.1 Materials

Electrospun NRL/PVA nanofibres prepared in previous studies were utilised (Osei *et al.*, 2022). AgNP-NRL/PVA nanofibre composites were prepared by adding 0.01 M and 0.015 M silver nitrate (AgNO₃) solutions to two separate NRL/PVA solutions. These solutions were electrospun to form two nanofibre sheets (nanofibre composites). The nanofibre composites were named 0.01 M AgNP and 0.015 M AgNP, according to the AgNO₃ concentration used in their syntheses. Nanoparticles in the 0.01 M AgNP were about 2.35 AgNP per 10 000 nm^2 area with an average size of 8.15 ± 0.09 nm. The 0.015 M AgNP were about 23.66 AgNP per 10 000 nm^2 area with an average size of 2.82 ± 0.04 nm. Nanoparticles of the 0.01 M AgNP were mostly located near or on the surface of the fibres. On the other hand, nanoparticles of the 0.015 M AgNP were mainly located within the fibre walls. Hydrochloric acid (HCl; 25.0%), nitric acid (HNO; 68.0%) and sodium hydroxide (NaOH; > 97%) were purchased from Merck, Brenntag Ghana Ltd. and Paskem Fine Chem Pvt. Ltd., respectively. Cadmium solutions used for adsorption studies were prepared from 1 000 mg/L Cd^{2+} standard solution purchased from pg Instruments.

2.2 Methods Used

2.2.1 Adsorption Study

At an ambient temperature of 27 °C, 5×5 cm^2 of 0.01 M and 0.015 M AgNP were placed in separate 50 mL Cd^{2+} solutions to determine how efficiently the nanofibre composites would adsorb Cd^{2+}. The solutions were shaken at 200 rpm on an orbital shaker. Contact time, pH and initial concentration were varied between 0 – 120 min, 4 – 7 and 0.01 – 1.00 ppm, respectively. After adsorption experiments, Cd^{2+} concentrations in solution were determined using an atomic absorption spectrophotometer (Shimadzu AA-7000). Removal efficiency and adsorption capacity of 0.01 M and 0.015 M AgNP were determined using Equations (1) and (2), respectively.

$$RE\ (\%) \ = \frac{C_o - C_e}{C_o} \times 100 \qquad (1)$$

$$q_e (mg/g) \ = \ \frac{(C_o - C_e) \cdot V}{m} \qquad (2)$$

where C_o (mg/L) = initial adsorbate concentration in solution, C_e (mg/L) = adsorbate concentration at equilibrium, V (L) = volume of adsorbate solution, and m (g) = mass of the AgNP in nanofibre composite used. Per calculations, 5×5 cm^2 (of 549.1504 cm^2, the total area electrospun for each nanofibre composite) of 0.01 M and 0.015 M AgNP nanofibre composites contain ~0.3929 mg and ~0.5893 mg of Ag, respectively.

2.2.2 Adsorption Isotherm

Data from the adsorption experiments were fitted to the Langmuir, Freundlich and Dubinin-Radushkevich (D-R) isotherms. This was done to understand the relationship between the adsorbent and the adsorbate in the solution (Sawyer *et al.*, 2003; Tran *et al.*, 2017). In the Langmuir isotherm, presented in Equation (3), all active sites of the adsorbent are assumed to have the same affinity for the adsorbate. The model is associated with a separation factor (R_L) which determines whether the adsorption is favourable or not (Equation 4) (Langmuir, 1918; Tran *et al.*, 2017).

$$q_e = \frac{q_{max} + (K_L \cdot C_e)}{1 + (K_L \cdot C_e)} \qquad (3)$$

$$R_L = \frac{1}{1 + (K_L \cdot C_o)} \qquad (4)$$

where q_{max} (mg/g) = the adsorbent's maximum capacity, and K_L (L/mg) = Langmuir constant. The adsorption is favourable if $0 < R_L < 1$ and unfavourable if $R_L > 1$. The adsorption may also be linear if $R_L = 1$ or irreversible if $R_L = 0$.

On the other hand, Freundlich isotherm, proposed by Freundlich (1906), assumes that the active sites of an adsorbent have different affinities for different adsorbates (Sawyer *et al.*, 2003). This is presented in Equation (5).

$$q_e = K_F \cdot C_e^{\frac{1}{n}} \qquad (5)$$

where K_F (mg/g)/(mg/L)$^{1/n}$ = Freundlich constant, and n = change in adsorption intensity with changes in the adsorption density. Depending on the value of 1/n, the adsorption may be favourable (1/n < 1) or unfavourable (1/n > 1)

The D-R isotherm is mainly applied to porous adsorbents. Since the matrix was porous, the D-R isotherm was employed to obtain additional information on the adsorption process. The D-R isotherm, as proposed by Dubinin and Radushkevich (1947), is presented in Equation (6), and its adsorption energy, E (kJ/mol), is also shown in Equation (7).

$$q_e = q_{DR} \cdot e^{(-K_{DR} \cdot \varepsilon^2)} \qquad (6)$$

$$E = \frac{1}{\sqrt{2 \cdot K_{DR}}} \qquad (7)$$

where q_{DR} (mg/g) = adsorption capacity, K_{DR} (mol^2/kJ^2) = constant related to sorption energy and ε (kJ/mol) = the Polanyi potential. Polanyi potential is computed as shown in Equation (8).

$$\varepsilon = RT \cdot \ln(1 + \frac{C^o}{C_e}) \qquad (8)$$

where R (8.314 × 10^{-3} kJ/mol·K) = universal gas constant, T (K) = temperature for adsorption and C^o (mg/g) = concentration of the adsorbate in standard state (1 mol/dm^3) (Zhou, 2020). At standard state, 1 mol/dm^3 = 112 411 mg/L for Cd^{2+}.

2.2.3   Adsorption Kinetics

Adsorption data were fitted to the pseudo-first order (PFO), pseudo-second order (PSO), Elovich and intra-particle diffusion kinetic models to elucidate the adsorption mechanisms and the rate of reaction. The PFO model is expressed as shown in Equation (9) (Lagergren, 1898).

$$q_t = q_e \cdot (1 - e^{-k_1 \cdot t}) \qquad (9)$$

where q_t (mg/g) = amount of adsorbate adsorbed at time t (min), and k_1 (1/min) = PFO equation's rate constant. Mostly, the PFO model can accurately describe the first 20 to 30 min of contact time and not beyond (Ho and McKay, 1998). The PSO kinetic model, which is also widely applied to adsorption

data, is presented in Equation (10) (Blanchard *et al.*, 1984).

$$q_t = \frac{k_2 (q_e)^2 t}{1 + (k_2 q_e t)} \qquad (10)$$

where k_2 (g/(mg × min)) = PSO equation's rate constant.

The Elovich kinetic model, proposed by Roginsky and Zeldovich (1934), is mainly applied to chemical adsorption data (Tran *et al.*, 2017). As expressed in Equation (11), the Elovich kinetic model provides insight into the desorption constant of the adsorption (β; g/mg) and the initial rate constant (α; mg/(g × min)). The model is as follows:

$$q_t = \frac{1}{\beta} \ln(1 + \alpha \beta t) \qquad (11)$$

Finally, the intra-particle diffusion model, proposed by Weber and Morris (1963), can predict the reaction pathway and adsorption mechanism (Tran *et al.*, 2017). The model is presented in Equation (12).

$$q_t = k_p \sqrt{t} + C \qquad (12)$$

where k_p (mg/(g × min$^{1/2}$)) = diffusion rate constant, and C (mg/g) = constant associated to the boundary layer's thickness.

2.2.4   Metal Concentration in Solution

Before and after adsorption studies, Cd^{2+} concentration was determined using the Flame AAS (FAAS; Shimadzu AA 7000). Five per cent HNO_3 (7.54 M) was added to the Cd^{2+} solution prior to FAAS analysis, according to APHA 3111B standard method. This method was also applied in analysing Ag concentration after treating the contaminated water with the nanofibre composites.

2.2.5 Morphology and Elemental Composition of the Nanofibre Composite After Adsorption

Morphology of the nanofibre composites was examined using a scanning electron microscope (SEM; Zeiss EVO MA 15) before and after adsorption. The SEM was equipped with an energy dispersive x-ray spectrometer (EDS; Bruker) which was used to determine if the nanocomposite had truly adsorbed Cd^{2+} after the adsorption process.

3 Results and Discussion

3.1 Effect of pH

A solution's pH can significantly affect the surface chemistry of adsorbate and adsorbent, hence,

affecting adsorption. Fig. 1 shows how pH affects Cd^{2+} adsorption by the AgNP-NRL/PVA nanofibre composites. The initial concentration was maintained at 1.00 ppm; contact time was maintained at 20 min and 40 min for 0.01 M and 0.015 M AgNP, respectively, whilst pH was varied between 4 – 9. From Fig. 1, it can be seen that the amount of Cd^{2+} removed by 0.01 M AgNP gradually increased from 4.41 mg/g, representing 3.33%, at pH 4 to 39.82 mg/g, representing 30.04%, at pH 7. After pH 7, the amount of Cd^{2+} removed reduced from 39.82 mg/g to below detection at pH 9. For 0.015 M AgNP, a similar trend was recorded: the amount of Cd^{2+} removed increased from 2.94 mg/g, representing 3.33%, at pH 4 to 29.49 mg/g, representing 33.67%, at pH 7. After this, there was a gradual decrease in Cd^{2+} adsorbed from 29.49 mg/g (33.67%) at pH 7 to 3.83 mg/g, representing 4.32%, at pH 9.

The observed trend was similar to that of other researchers, such as Jiang *et al.* (2006), where maximum amount of Cd^{2+} removed from an aqueous solution occurred at pH 7. On the other hand, in a study by Al-Qahtani (2017) where AgNP synthesised using *Benjamina* leaf extracts was used to adsorb Cd^{2+} from solution, the maximum uptake of Cd^{2+} occurred at pH 6, with a decrease in uptake recorded at pH 7. Observations in this study contradicts that of Al-Qahtani (2017), with maximum uptake occurring at pH 7, whilst a sharp decrease in uptake was observed at pH 8.

It is worth mentioning that according to the Pourbaix diagrams of Takeno (2005), at pH 7 and Eh of 0.22 V (SHE), Cd exists as Cd^{2+}. This explains why relatively lower adsorption of Cd^{2+} was recorded at lower pH, such as 4 and 5. At lower pH, cation adsorption is limited because H^+ is more readily and directly adsorbed onto surfaces than other cations (Drever, 1997).
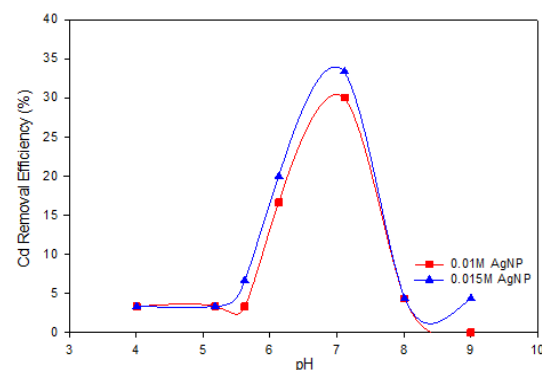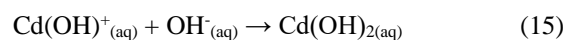
On the other hand, at around pH 7, H^+ in the solution becomes limited, enabling Cd^{2+} to bond freely to the adsorbent. Also, according to Henglein (1998), Cd^{2+} adsorption could be ascribed to the cathodic charging of AgNP, which causes Cd^{2+} to reduce on the AgNP surface (Equation 13).

$$Ag_x{}^{(y+2)-} + Cd^{2+} \rightarrow (Ag_xCd)^{y-} \quad (13)$$
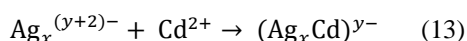
where x = number of Ag clusters and y = moles of Ag^+ in the AgNP synthesis reaction (yAg^+). The AgNP can serve as a cathode for deposition due to its higher standard electrode potential than Cd (Ag^+/Ag^o (0.80 V); Cd^{2+}/Cd^o (-0.40 V)).

However, OH^- ions may become abundant when an alkali region is formed, that is, pH beyond 7. Hence Cd^{2+} may readily form $Cd(OH)^+{}_{(aq)}$ and $Cd(OH)_{2\ (aq)}$,

therefore limiting Cd^{2+} adsorption (Equations (14) and (15)). This probably caused the decrease in per cent of Cd^{2+} adsorbed at pH beyond 7.

$$Cd^{2+}{}_{(aq)} + OH^-{}_{(aq)} \rightarrow Cd(OH)^+{}_{(aq)} \quad (14)$$

$$Cd(OH)^+{}_{(aq)} + OH^-{}_{(aq)} \rightarrow Cd(OH)_{2(aq)} \quad (15)$$

Fig. 1 Effect of pH on Cd^{2+} Adsorption by AgNP-NRL/PVA Nanofibre Composites

3.2 Effect of Contact Time

How long an adsorbate solution remains in contact with an adsorbent determines the optimum adsorption efficiency. At a pH of 7 and an initial concentration of 1.00 ppm, the effect of contact time on Cd^{2+} adsorption was studied, ranging from 0 – 120 min. Fig. 2 presents the effect of contact time on Cd^{2+} adsorption by NRL/PVA only and AgNP-NRL/PVA nanofibre composites.

By comparing the removal efficiency of NRL/PVA only, which does not contain AgNP, to that of 0.01 M and 0.015 M AgNP, it can be seen that NRL/PVA adsorbed a relatively smaller amount of Cd^{2+}. This signifies that the AgNP in AgNP-NRL/PVA nanofibre composites improved Cd^{2+} removal from the aqueous solution. For 0.01 M AgNP, maximum amount of Cd^{2+} was removed at 20 min, representing 14.9674 mg/g (11.90%), which later decreased with an increase in uptake at 120 min. On the other hand, the maximum uptake of Cd^{2+} for 0.015 M AgNP occurred at 40 min, representing 30.1129 mg/g (35.92%), with a slight drop in uptake at 60 min. The maximum uptake recorded at 40 min for 0.015 M AgNP was similar to that recorded by Al-Qahtani (2017). However, Jiang *et al.* (2006) observed the maximum uptake of Cd^{2+} by tourmaline at 60 min.

From Fig. 2, it can be seen that the adsorption of Cd^{2+} by 0.015 M AgNP was relatively better than 0.01 M AgNP. This could be attributed to the fact that there are more AgNP in 0.015 M than in 0.01 M AgNP; hence the availability of relatively more active sites in 0.015 M AgNP for Cd^{2+} adsorption.

Also, from Equation (13), it can be seen that the higher the moles of Ag^+ (yAg^+), the higher the charge of the reduced complex formed $((Ag_xCd)^{y-})$. It is also worth mentioning that the higher the magnitude of the charge of the reduced complex, the stronger its attraction will be. Hence, better adsorption was observed in 0.015 M AgNP than in 0.01 M AgNP. The relatively smaller amount of active sites in 0.01 M AgNP probably resulted in the desorption and readsorption of Cd^{2+} after 20 min and at 120 min, respectively.
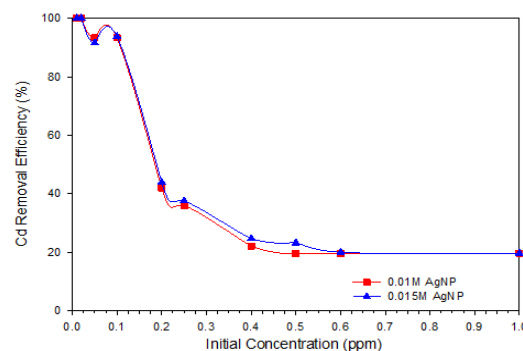
3.3 Effect of Initial Concentration

How concentration of Cd^{2+} in an aqueous solution affects its adsorption by AgNP-NRL/PVA nanofibre composites was studied. Whilst pH was held constant at 7, time at 20 min for 0.01 M AgNP and 40 min for 0.015 M AgNP, the initial concentration of Cd^{2+} was varied between 0.00 – 1.00 ppm. Results on how initial Cd^{2+} concentration affects adsorption by the nanofibre composites are presented in Fig. 3. It can be seen that maximum uptake occurred at 0.05 ppm (93.40%), with a minor drop in uptake at 0.10 ppm (93.30%) for Cd^{2+} adsorption by 0.01 M AgNP. One of the highest percentages of Cd^{2+} removed by 0.015 M AgNP occurred at 0.10 ppm (93.80%), similar to Cd^{2+} adsorption by 0.01 M AgNP. A significant drop in Cd^{2+} adsorbed by both nanofibre composites was recorded at 0.20 ppm (0.01 M AgNP = 27.00%; 0.015 M AgNP = 28.50%).
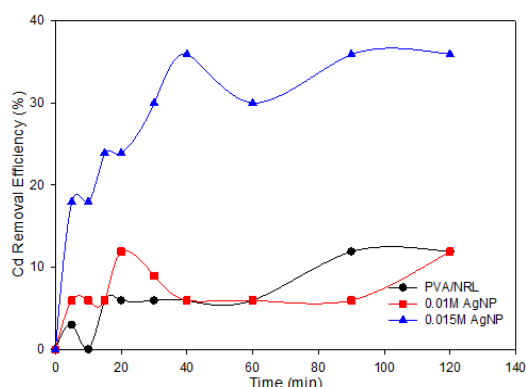
Fig. 2 Effect of Contact Time on Cd^{2+} Adsorption by NRL/PVA and AgNP-NRL/PVA Nanofibre Composites

This was followed by a gradual decrease in the percentage of Cd^{2+} removed until 1.00 ppm (0.01 M AgNP = 19.68%; 0.015 M AgNP = 19.68%). The gradual decrease in Cd^{2+} adsorbed by both nanofibre composites was due to the relatively smaller number of active sites available for adsorption as the initial concentration increased.


Fig. 3 Effect of Initial Concentration on Cd^{2+} Adsorption by AgNP-NRL/PVA Nanofibre Composites

3.4 Adsorption Isotherm

Fig. 4 presents the Langmuir, Freundlich and D-R isotherms for Cd^{2+} adsorption by 0.01 M and 0.015 M AgNP. The experimental data were fitted to the aforementioned models to understand the adsorption behaviour between Cd^{2+} on the surfaces of the nanofibre composites. Table 1 shows the adsorption isotherm model parameters as well as their respective coefficient of determination (R^2) and mean square error (MSE) for Cd^{2+} adsorption by 0.01 M and 0.015 M AgNP. The adsorption data for both nanofibre composites were a weak fit to Langmuir isotherm. However, for both nanofibre composites, the experimental data were a good fit to D-R isotherm but the best fit to the Freundlich isotherm with 0.01 M AgNP having an R^2 and MSE values of 0.7413 and 10.5678 $(mg/g)^2$, respectively. The nanofibre composite, 0.015 M AgNP, had R^2 and MSE values of 0.8066 and 3.6705 $(mg/g)^2$, respectively.

The adsorption data fitting best to the Freundlich isotherm means the adsorbates formed a multi-layer on the surface of the adsorbent. Since 1/n values for 0.01 M (0.2245) and 0.015 M AgNP (0.2315) were greater than 0 but less than 1, it showed that the adsorption was favourable. As expressed in Equation (13), it is possible that as Cd^{2+} bonded with Ag to form an alloy, $(Ag_xCd)^{y-}$, and the negatively charged alloy promoted further adsorption of Cd^{2+} at the surface, hence the multilayered adsorption. Also, since in Freundlich isotherm, it is assumed that active sites available for adsorption have different affinities for the adsorbate, AgNP within the fibre may have contributed to the varied affinities across the surface of the nanofibre composites, resulting in Cd^{2+} multilayered adsorption. Though in general, 0.015 M AgNP adsorbed Cd^{2+} better than 0.01 M AgNP, the higher q_{DR} value of 0.01 M AgNP (47.7059 mg/g) than 0.015 M AgNP (35.4335 mg/g) means 0.01 M AgNP could have adsorbed more Cd^{2+} if the experiment's time frame had been

15

increased. The parameter E, which represents the adsorption energy, and may suggest whether the adsorption was physical or chemical was 20.8791 kJ/mol for 0.01 M AgNP and 20.3996 kJ/mol for 0.015 M AgNP. It is worth mentioning that the E values of both nanofibre composites were beyond the range for physical (< 8 kJ/mol) and chemical adsorption (8 – 16 kJ/mol) (Das *et al.*, 2013; Maneechakr and Mongkollertlop, 2020). Therefore, further studies may be required to understand the adsorption behaviour better.
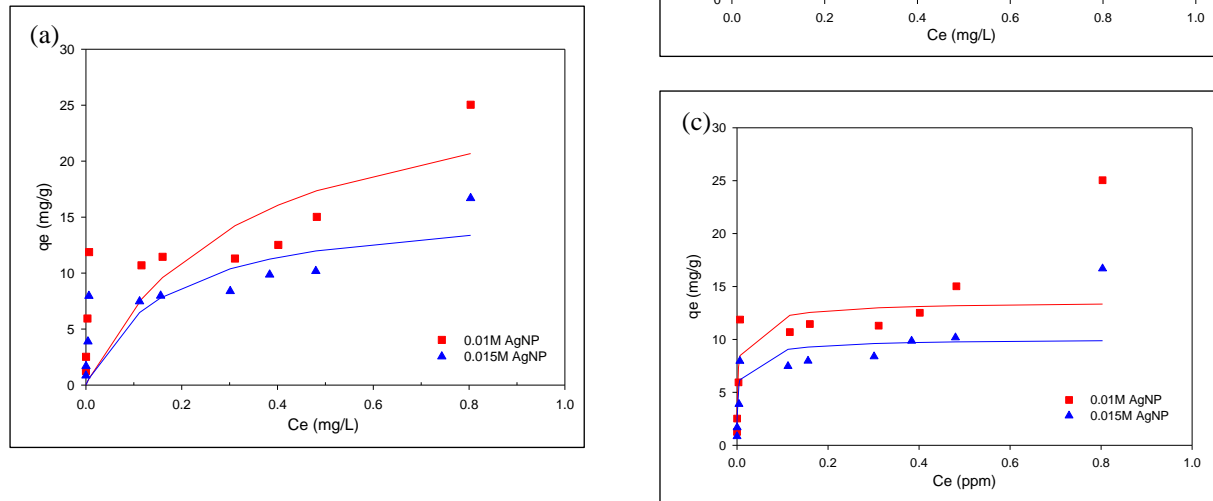
Fig. 4 (a) Langmuir (b) Freundlich and (c) Dubinin-Radushkevich Isotherm for the Adsorption of Cd^{2+} by 0.01 M and 0.015 M AgNP

Table 1 Parameters of Adsorption Isotherms for the Adsorption of Cd^{2+} by 0.01 M and 0.015 M AgNP

Adsorbent	Langmuir parameters		R_L	R^2	MSE $[(mg/g)^2]$	Freundlich parameters		R^2	MSE $[(mg/g)^2]$
	q_{max} (mg/g)	K_L (L/mg)				1/n	K_F $[(mg/g)/(mg/L)^{1/n}]$		
0.01 M AgNP	28.9897	3.0981	0.2440-0.9700	0.4483	22.5407	0.2245	19.2994	0.7413	10.5678
0.015 M AgNP	16.1689	5.9596	0.1437-0.9438	0.5187	9.1348	0.2315	13.6678	0.8066	3.6705

Adsorbent	D-R parameters			R^2	MSE $[(mg/g)^2]$
	q_{DR} (mg/g)	K_{DR} (mol^2/kJ^2)	E (kJ/mol)		
0.01 M AgNP	47.7059	0.0011	20.8791	0.7238	11.2840
0.015 M AgNP	35.4335	0.0012	20.3996	0.7904	3.9789

3.5 Adsorption Kinetics

The adsorption data were fitted to the PFO, PSO, Elovich and intra-particle diffusion models to understand the reaction rate and adsorption mechanism. Fig. 5 shows the plot f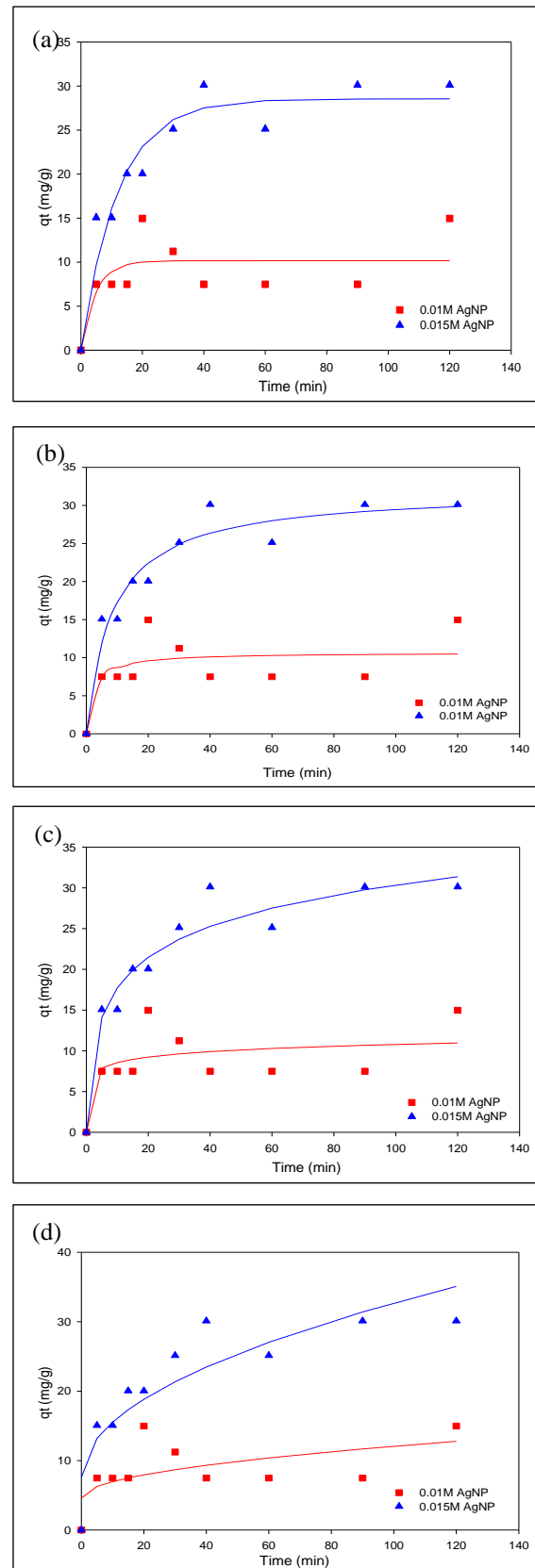or the four adsorption kinetic models, and Table 2 shows the parameters of the kinetic models. The experimental data for Cd^{2+} adsorption by 0.01 M AgNP was a weak fit to the PFO ($R^2 = 0.5384$; MSE = 7.8203 $(mg/g)^2$), PSO ($R^2 = 0.5349$; MSE = 7.8790 $(mg/g)^2$) and Elovich ($R^2 = 0.5338$; MSE = 7.8978 $(mg/g)^2$) kinetic models and a poor fit to the intra-particle diffusion model ($R^2 = 0.3333$; MSE = 11.2950 $(mg/g)^2$). Although Cd^{2+} adsorption by 0.01 M AgNP fitted best to the PFO kinetic model, which

16

represents physical adsorption, its experimental data fitted best to Freundlich isotherm, which represents chemical adsorption. The discrepancy observed was likely due to the weak fit of the experimental data to the PFO model, hence not adequately describing the type of adsorption taking place. The poor and weak fit of Cd^{2+} adsorption by 0.01 M AgNP data to all four kinetic models used in this study might have been due to the desorption of Cd^{2+} recorded after 20 min and subsequent readsorption at 120 min. This implies that the experiment should have been cut short at 20 min or extended beyond 120 min to obtain more precise information about the adsorption kinetics. Also, Tran *et al.* (2017) and Revellame *et al.* (2020) explains that stopping an experiment before reaching equilibrium or including experimental data after reaching equilibrium can result in wrong inferences.

For Cd^{2+} adsorption using 0.015 M AgNP, the experimental data were a good fit to the PFO (R^2 = 0.9214; MSE = 6.2582 $(mg/g)^2$), PSO (R^2 = 0.9443; MSE = 4.4371 $(mg/g)^2$), and intra-particle diffusion (R^2 = 0.8006; MSE = 15.8823 $(mg/g)^2$) kinetic models. The best fit was for the Elovich kinetic model (R^2 = 0.9461; MSE = 4.2957 $(mg/g)^2$). Since Freundlich isotherm and Elovich kinetic model best describes Cd^{2+} adsorption by 0.015 M AgNP, it could be that chemisorption might have occurred during the adsorption process. The Elovich model also showed that the initial rate of adsorption of Cd^{2+} by 0.015 M AgNP (α = 12.8106 mg/(g $\times$ min)) was slower than that of 0.01 M AgNP (α = 679.0428 mg/(g $\times$ min)). However, the desorption constant showed that a relatively smaller amount of Cd^{2+} will desorb from 0.015 M AgNP (β = 0.1793 g/mg) than from 0.01 M AgNP (β = 1.0351 g/mg) within the experiment's time frame. Also, from the intra-particle diffusion model, 0.015 M AgNP (C = 7.5959 mg/g) had a relatively larger boundary layer for adsorption than 0.01 M AgNP (C = 4.5942 mg/g). From this, it can be inferred that the presence of relatively more AgNP in 0.015 M AgNP (due to the relatively higher yAg$^+$) resulted in the larger boundary layer and lower desorption constant; hence, the better adsorption observed in 0.015 M AgNP.

3.6 Elemental Composition of AgNP-NRL/PVA After Adsorption

Fig. 6 shows an SEM image of AgNP-NRL/PVA nanofibre composite and its corresponding EDS spectra before Cd^{2+} adsorption. The whitish specks in Fig. 6a are the AgNP clusters on the nanofibre composite. Its EDS spectra (Fig. 6b) confirm these white specks as AgNP clusters. Fig. 7 shows an SEM image of AgNP-NRL/PVA nanofibre composite and its corresponding EDS spectra after Cd^{2+} adsorption.

Fig. 5 (a) Pseudo-First Order (b) Pseudo-Second Order (c) Elovich and (d) Intra-Particle Diffusion Kinetic Models for the Adsorption of Cd^{2+} by 0.01 M and 0.015 M AgNP
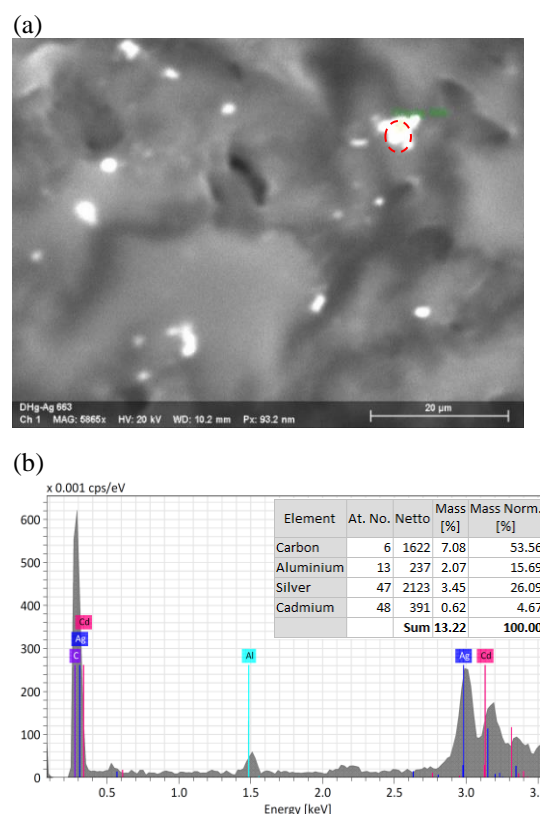
Table 2 Parameters of Adsorption Kinetics for the Adsorption of Cd^{2+} by 0.01 M and 0.015 M AgNP

Model	Parameters	Adsorbent	
		0.01 M AgNP	*0.015 M AgNP*
PFO	q_e (mg/g)	10.1604	28.5447
	k_1 (1/ min)	0.2074	0.0831
	R^2	0.5384	0.9214
	MSE [(mg/g)^2]	7.8203	6.2582
PSO	q_e (mg/g)	10.6641	31.9701
	k_2 [g/(mg × min)]	0.0416	0.0037
	R^2	0.5349	0.9443
	MSE [(mg/g)^2]	7.8790	4.4371
Elovich	α [mg/(g × min)]	679.0428	12.8106
	β (g/mg)	1.0351	0.1793
	R^2	0.5338	0.9461
	MSE [(mg/g)^2]	7.8978	4.2957
Intra-particle diffusion	k_p [mg/(g × min$^{1/2}$)]	0.7467	2.5093
	C (mg/g)	4.5942	7.5959
	R^2	0.3333	0.8006
	MSE [(mg/g)^2]	11.2950	15.8823

(a)

(b)
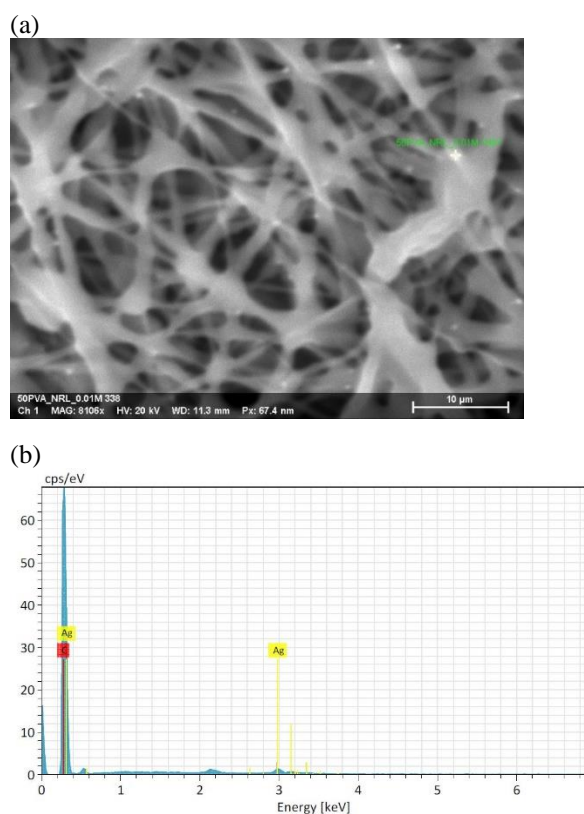
Fig. 6 (a) BSD-SEM Image with (b) EDX Analysis Before the Adsorption of Cd^{2+} by AgNP-NRL/PVA Nanofibre Composite

(a)

(b)

Element	At. No.	Netto	Mass [%]	Mass Norm. [%]
Carbon	6	1622	7.08	53.56
Aluminium	13	237	2.07	15.69
Silver	47	2123	3.45	26.09
Cadmium	48	391	0.62	4.67
		Sum	13.22	100.00

Fig. 7 (a) BSD-SEM Image with (b) EDX Analysis After the Adsorption of Cd^{2+} by AgNP-NRL/PVA Nanofibre Composite

Similar to Fig. 6a, the whitish specks in Fig. 7a also represent AgNP clusters. From Fig. 7a, it can be seen that upon removal of the nanofibre composite from the aluminium foil (substrate for collecting nanofibres during electrospinning) and when in contact with water, the nanofibres collapse and clamp together, forming larger and fewer pores as seen in Fig. 7a (Osei *et al.*, 2022).

The EDS analysis of the red circled area in Fig 7a is shown in Fig. 7b. It can be seen from the EDS spectra that Cd^{2+} is present where AgNP clusters are. This shows that the nanoparticles had indeed removed Cd^{2+} from the aqueous solution. The presence of aluminium in the spectra was likely due to fragments of the aluminium foil sticking to the nanofibre composite during its removal (Osei *et al.*,

2022) because aluminium foil was used to support the matrix nanocomposite during electrospinning.

3.7 Silver (Ag) Released into Solution After Water Treatment

After the adsorption study, it was necessary to determine the amount of Ag released into solution. Since AgNP was synthesised to remove Cd^{2+} from contaminated water, it would not be ideal for excess Ag to be released into the water and become part of the contamination problem. The amount of Ag released into solution after Cd^{2+} adsorption by the AgNP-NRL/PVA and guidelines values for Ag in drinking water are presented in Tables 3 and 4, respectively. According to both the US Environmental Protection Agency (US EPA) and the World Health Organisation (WHO), Ag in drinking water should not exceed 0.10 mg/L (Table 4). Table 3 shows that 0.01 M and 0.015 M AgNP released 0.0425 mg/L and 0.0510 mg/L of Ag into the solution, which is less than the US EPA and WHO guidelines. This means Ag released into the water would not pose detrimental effect upon human usage.

Table 3 Ag Concentration in Solution After Cd^{2+} Adsorption

Fibre Matrix (AgNP)	Ag Concentration (mg/L)
0.01 M	0.0425
0.015 M	0.0510

Table 4 Guidelines for Ag Concentration in Drinking Water

Guideline/Standard	Ag Concentration (mg/L)	Reference
US EPA SMCL*	0.1000	(Anon., 2013)
WHO-drinking water	0.1000	(Anon., 2011)

*Secondary Maximum Contaminant Level

Since the matrix for AgNP synthesis, that is, NRL/PVA, is partially soluble, the surfaces of the fibres bearing AgNP might have dissolved into the solution. Hence, accounting for the Ag concentrations recorded. It is also worth mentioning that Ag released by 0.015 M AgNP was greater than that of 0.01 M AgNP due to the higher molar ratio of Ag in 0.015 M AgNP.

4 Conclusion

The efficiency of AgNP in electrospun NRL/PVA nanofibre matrix (0.01 M and 0.015 M AgNP) to remove Cd^{2+} from contaminated water has been investigated. Factors such as pH, contact time, and initial Cd^{2+} concentration that play a critical role in sorption processes were considered. For both adsorbents, the maximum uptake of Cd^{2+} occurred at pH 7 and around 20 min for 0.01 M AgNP (14.9674 mg/g; 11.90%) and 40 min for 0.015 M AgNP (30.1129 mg/g; 35.92%). As the initial Cd^{2+} concentration increased, the nanofibre composites' removal efficiency decreased, and the adsorption probably resulted in Cd^{2+} forming an alloy with Ag. The experimental data for Cd^{2+} adsorption by 0.01 M and 0.015 M AgNP fitted best to Freundlich isotherm, implying that the adsorption occurred in a multilayered fashion. For the adsorption kinetics of Cd^{2+}, the experimental data for adsorption by 0.01 M AgNP was poor and weak fit to all kinetic models utilised in this study. This showed that the time range selected was inappropriate for Cd^{2+} adsorption by 0.01 M AgNP. Hence, the experiment must be stopped at 20 min or extended beyond 120 min to understand its kinetics better.

On the other hand, the adsorption data of Cd^{2+} by 0.015 M AgNP was a good fit to the Elovich kinetic model, showing that Cd^{2+} was chemically adsorbed. In general, 0.015 M AgNP adsorbed Cd^{2+} better than 0.01 M AgNP, and this was plausible because of its lower desorption constant (β = 0.1793 g/mg) and larger boundary layer (C = 7.5959 mg/g) than 0.01 M AgNP (β = 1.0351 g/mg; C = 4.5942 mg/g). The better efficiency of 0.015 M AgNP was mainly due to relatively higher number of AgNP present in the nanofibre for adsorption as well as higher molar ratio of Ag^+ in 0.015 M AgNP during its synthesis. SEM and EDS analysis confirmed that the nanofibre composite had adsorbed Cd^{2+} from the aqueous solution. After the adsorption process, the concentration of Ag released into the treated water was below US EPA and WHO limits of 0.10 mg/L for both 0.01 M AgNP (0.0425 mg/L) and 0.015 M AgNP (0.0510 mg/L), which renders the water safe in terms of Ag contamination.

Utilising these nanofibre composites as an adsorbent for Cd^{2+} removal in contaminated water is promising since the methodology is simple, and the materials used are readily available locally. Also, since the concentration of Ag released into the treated water is not detrimental to health, no further treatment process may be required to reduce or eliminate Ag in this water. Therefore, further research would be necessary in order to enhance the efficiency of the AgNP-NRL/PVA in adsorbing Cd^{2+} from an aqueous solution since this adsorbent looks promising.

Acknowledgement

References

Al-Qahtani, K. M. (2017), "Cadmium Removal from Aqueous Solution by Green Synthesis Zero Valent Silver Nanoparticles with *Benjamina* Leaves Extract", *Egyptian Journal of Aquatic Research,* Vol. 43, No. 4, pp. 269-274.

Anon. (2011), *Guidelines for Drinking-Water Quality*, 4th edition, World Health Organisation, Malta, 541 pp.

Anon. (2013), *Silver*, Water Quality Association, Illinois, 3 pp.

Aoshima, K. (2012), "Itai-Itai Disease: Cadmium-Induced Renal Tubular Osteomalacia", *Japanese Journal of Hygiene*, pp. 455-463.

Aoshima, K. (2016), "Itai-Itai Disease: Renal Tubular Osteomalacia Induced by Environmental Exposure to Cadmium - Historical Review and Perspectives", *Soil Science and Plant Nutrition,* Vol. 62, No. 4, pp. 319-326.

Balali-Mood, M., Naseri, K., Tahergorabi, Z., Khazdair, M. R. and Sadeghi, M. (2021), "Toxic Mechanisms of Five Heavy Metals: Mercury, Lead, Chromium, Cadmium, and Arsenic", *Frontiers in Pharmacology,* Vol. 12, p. 643972.

Blanchard, G., Maunaye, M. and Martin, G. (1984), "Removal of Heavy Metals from Waters by Means of Natural Zeolites", *Water Research,* Vol. 18, No. 12, pp. 1501-1507.

Colantonio, N. and Kim, Y. (2016), "Cadmium (Ii) Removal Mechanisms in Microbial Electrolysis Cells", *Journal of Hazardous Materials,* Vol. 311, pp. 134-141.

Das, B., Mondal, N. K., Bhaumik, R. and Roy, P. (2013), "Insight into Adsorption Equilibrium, Kinetics and Thermodynamics of Lead onto Alluvial Soil", *International Journal of Environmental Science and Technology,* Vol. 11, No. 4, pp. 1101-1114.

Drever, J. I. (1997), "Adsorption", In Chap. 5 of *The Geochemistry of Natural Waters: Surface and Groundwater Environments,* 3rd edition, Prentice Hall, New Jersey, pp. 87-105.

Dubinin, M. M. and Radushkevich, L. V. (1947), "The Equation of the Characteristic Curve of Activated Charcoal", *Proceedings of the Academy of Sciences of the USSR: Physical Chemistry Section,* Vol. 55, pp. 331-337.

Elkhatib, E., Mahdy, A., Sherif, F. and Elshemy, W. (2016), "Competitive Adsorption of Cadmium (Ii) from Aqueous Solutions onto Nanoparticles of Water Treatment Residual", *Journal of Nanomaterials,* Vol. 2016, pp. 1-10. p. 1.

Freundlich, H. (1906), "Over the Adsorption in Solution", *Journal of Physical Chemistry,* Vol. 57, pp. 385-471.

Han, T. Y., Chang, S. H., Lee, H. K. and Son, S.-J. (2011), "Successful Treatment of Argyria Using a Low-Fluence Q-Switched 1064-nm Nd:YAG Laser", *International Journal of Dermatology,* Vol. 50, No. 6, pp. 751-753.

Henglein, A. (1998), "Colloidal Silver Nanoparticles: Photochemical Preparation and Interaction with O_2, CCl_4, and Some Metal Ions", *Chemistry of Materials,* Vol. 10, pp. 444-450.

Ho, Y. S. and McKay, G. (1998), "A Comparison of Chemisorption Kinetic Models Applied to Pollutant Removal on Various Sorbents", *Trans IChemE,* Vol. 76, No. Part B, pp. 332-340.

Jiang, K., Sun, T.-H., Sun, L.-N. and Li, H.-b. (2006), "Adsorption Characteristics of Copper, Lead, Zinc and Cadmium Ions by Tourmaline", *Journal of Environmental Sciences,* Vol. 18, No. 6, pp. 1221-1225.

Kango, S. and Kumar, R. (2016), "Magnetite Nanoparticles Coated Sand for Arsenic Removal from Drinking Water", *Environmental Earth Sciences,* Vol. 75, No. 5, pp. 1-12.

Lagergren, S. (1898), "About the Theory of So-Called Adsorption of Soluble Substances", *Kungliga Svenska Vetenskapsakademiens Handlingar,* Vol. 24, No. 4, pp. 1-39.

Langmuir, I. (1918), "The Adsorption of Gases on Plane Surfaces of Glass, Mica and Platinum", *Journal of the American Chemical Society,* Vol. 40, No. 9, pp. 1361-1403.

Mahmood, Q., Asif, M., Shaheen, S., Hayat, M. T. and Ali, S. (2019), "Cadmium Contamination in Water and Soil", In Chap. 6 of *Cadmium Toxicity and Tolerance in Plants*, Elsevier, pp. 141-161.

Maneechakr, P. and Mongkollertlop, S. (2020), "Investigation on Adsorption Behaviors of Heavy Metal Ions (Cd^{2+}, Cr^{3+}, Hg^{2+} and Pb^{2+}) through Low-Cost/Active Manganese Dioxide-Modified Magnetic Biochar Derived from Palm Kernel Cake Residue", *Journal of Environmental Chemical Engineering,* Vol. 8, No. 6, pp. 1-9.

Osei, L. B., Ndur, S. A. and Fosu, S. (2022), "Synthesis and Characterisation of Electrospun Natural Rubber Latex/Polyvinyl Alcohol for Application in Aqueous Processes", *Journal of Rubber Research,* Vol. 25, pp. 313-320.

Pietroiusti, A., Stockmann-Juvala, H., Lucaroni, F. and Savolainen, K. (2018), "Nanomaterial Exposure, Toxicity and Impact on Human Health", *Wiley Interdisciplinary Reviews: Nanomedicine and Nanobiotechnology,* Vol. 10, No. 5, pp. 1-21.

Revellame, E. D., Fortela, D. L., Sharp, W., Hernandez, R. and Zappi, M. E. (2020), "Adsorption Kinetic Modeling Using Pseudo-First Order and Pseudo-Second Order Rate Laws: A Review", *Cleaner Engineering and Technology,* Vol. 1, pp. 1-13.

Roginsky, S. and Zeldovich, Y. B. (1934), "The Catalytic Oxidation of Carbon Monoxide on Manganese Dioxide", *Acta Physico-Chemica USSR,* Vol. 1, p. 554.

Roksana, M. (2016), "Eco-Friendly Alternative for Water Treatment from Nanotechnology", *Journal Nano Science and Technology,* Vol. 4, pp. 28-34.

Sahu, S. C. and Hayes, W. (2017), "Toxicity of Nanomaterials Found in Human Environment: A Literature Review", *Toxicology Research and Application,* Vol. 1, pp. 1-13.

Salehi, M., Li, X. and Whelton, A. J. (2017), "Metal Accumulation in Representative Plastic Drinking Water Plumbing Systems", *Journal - American Water Works Association,* Vol. 109, No. 11, pp. 479-493.

Sawyer, C. N., McCarty, P. L. and Parkin, G. F. (2003), *Chemistry for Environmental Engineering and Science*, 5th edition, McGraw Hill Education, New Dehli, 752 pp.

Shao-Feng, N., Yong, L., Xin-Hua, X. and Zhang-Hua, L. (2005), "Removal of Hexavalent Chromium from Aqueous Solution by Iron Nanoparticles", *Journal of Zhejiang University Science,* Vol. 6, No. 10, pp. 1022-1027.

Takeno, N. (2005), *Atlas of Eh-Ph Diagrams: Intercomparison of Thermodynamic Database. Geological Survey of Japan Open File Report No.419*, National Institute of Advanced Industrial Science and Technology, Research Center for Deep Geological Environments, 285 pp.

Tauanov, Z., Tsakiridis, P. E., Shah, D. and Inglezakis, V. J. (2019), "Synthetic Sodalite Doped with Silver Nanoparticles: Characterisation and Mercury (Ii) Removal from Aqueous Solutions", *Journal of Environmental Science and Health, Part A Toxic/Hazardous Substances and Environmental Engineering,* Vol. 54, No. 9, pp. 951-959.

Tavker, N., Yadav, V. K., Yadav, K. K., Cabral-Pinto, M. M., Alam, J., Shukla, A. K., Ali, F. A. A. and Alhoshan, M. (2021), "Removal of Cadmium and Chromium by Mixture of Silver Nanoparticles and Nano-Fibrillated Cellulose Isolated from Waste Peels of Citrus Sinensis", *Polymers (Basel),* Vol. 13, No. 2.

Tchounwou, P. B., Yedjou, C. G., Patlolla, A. K. and Sutton, D. J. (2012), "Heavy Metal Toxicity and the Environment", *Experientia Supplementum,* Vol. 101, pp. 133-164.

Tran, H. N., You, S. J., Hosseini-Bandegharaei, A. and Chao, H. P. (2017), "Mistakes and Inconsistencies Regarding Adsorption of Contaminants from Aqueous Solutions: A Critical Review", *Water Research,* Vol. 120, pp. 88-116.

Weber, W. J. and Morris, J. C. (1963), "Kinetics of Adsorption on Carbon from Solution", *Journal of the Sanitary Engineering Division,* Vol. 89, No. 2, pp. 31-60.

Zhou, X. (2020), "Correction to the Calculation of Polanyi Potential from Dubinnin-Rudushkevich Equation", *Journal of Hazardous Materials,* Vol. 384, p. 121101.

Authors

Linda Bentuma Osei is a postgraduate assistant and PhD student at the University of Mines and Technology (UMaT), Ghana. She holds a BSc (Hons) in Environmental and Safety Engineering from UMaT. She is a member of the Ghana Institute of Safety and Environmental Professionals (GhISEP). Her research interests include nanofibre and nanoparticle synthesis and its application, water and wastewater treatment, heavy metal contamination in soils and environmental monitoring.

Shadrack Fosu holds a PhD degree in Minerals and Materials Engineering from The University of South Australia (UniSA), Adelaide-Australia and a BSc (Hons) degree in Minerals Engineering from the University of Mines and Technology (UMaT), Tarkwa-Ghana. He is currently a Senior Lecturer with the Environmental and Safety Engineering Department at UMaT. His research interest is in the area of Ore Characterisation and Process Mineralogy, Mineral Processing (Flotation and Aqueous Metallurgy), Simulation and Computer-aided Process Control and Instrumentation, Environmental Chemistry, Environmental Pollution, Water and Wastewater Treatment. He is a Fellow of West African Institute of Mining, Metallurgy and Petroleum (WAIMM) and member of International Association of Engineers (MIAENG).

Samuel Agyarko Ndur is an Associate Professor of Environmental and Safety Engineering currently working at the University of Mines and Technology (UMaT), Ghana. He holds a PhD from New Mexico Institute of Mining and Technology, USA. He is a fellow of the The West African Institute of Mining, Metallurgy and Petroleum (WAIMM) and a member of International Association for Impact Assessment (IAIA) and a Society of Environmental Geochemistry and Health (SEGH). His research interests include arsenic sequestration, mine waste characterisation and management, environmental impact assessment, corporate social responsibility, environmental monitoring and geochemistry.
.